JOURNAL OF PETROLOGY | VOLUME 47 | NUMBER 12 | PAGES 2357–2368 | 2006 | doi:10.1093/petrology/egl047

Recalibration of the Garnet–Muscovite (GM) Geothermometer and the Garnet–Muscovite–Plagioclase–Quartz (GMPQ) Geobarometer for Metapelitic Assemblages

CHUN-MING WU[1,2]* AND GUOCHUN ZHAO[2]

[1]LABORATORY OF COMPUTATIONAL GEODYNAMICS, THE GRADUATE SCHOOL, CHINESE ACADEMY OF SCIENCES, P.O. BOX 4588, BEIJING 100049, CHINA

[2]DEPARTMENT OF EARTH SCIENCES, THE UNIVERSITY OF HONG KONG, POKFULAM ROAD, HONG KONG, CHINA

RECEIVED NOVEMBER 27, 2005; ACCEPTED AUGUST 15, 2006; ADVANCE ACCESS PUBLICATION SEPTEMBER 21, 2006

The garnet–muscovite (GM) geothermometer and the garnet–muscovite–plagioclase–quartz (GMPQ) geobarometer have been simultaneously calibrated under conditions of $T = 450$–$760^\circ C$ and $P = 0{\cdot}8$–$11{\cdot}1$ kbar, using a large number of metapelitic samples in the compositional ranges $X_{Fe}^{grt} = 0{\cdot}53$–$0{\cdot}81$, $X_{Mg}^{grt} = 0{\cdot}05$–$0{\cdot}24$, $X_{Ca}^{grt} = 0{\cdot}03$–$0{\cdot}23$ in garnet, $X_{Ca}^{pl} = 0{\cdot}17$–$0{\cdot}74$ in plagioclase, and $Fe = 0{\cdot}04$–$0{\cdot}16$, $Mg = 0{\cdot}04$–$0{\cdot}13$, $Al^{VI} = 1{\cdot}74$–$1{\cdot}96$ in muscovite on the basis of 11 oxygens. The resulting GM thermometer yielded similar temperature estimates (mostly within $\pm 50^\circ C$) to that of the garnet–biotite thermometer, and successfully discerned the expected systematic temperature change of prograde sequences, thermal contact zones and an inverted metamorphic zone. The resulting GMPQ barometer yielded similar pressure estimates (mostly within $\pm 1{\cdot}0$ kbar) to the garnet–aluminum silicate–plagioclase–quartz (GASP) barometer and placed the aluminosilicate-bearing samples in the appropriate aluminosilicate stability fields. Application of the GMPQ barometer to thermal contact aureoles or rocks within limited geographical areas confirmed the expected constant pressures that should exist in these settings. The random errors of the GM thermometer and the GMPQ barometer are estimated to be $\pm 16^\circ C$ and $\pm 1{\cdot}5$ kbar, respectively. When biotite or aluminosilicate is absent in metapelites, metamorphic P–T conditions may be determined by simultaneously applying the GM thermometer and the GMPQ barometer.

KEY WORDS: *application; calibration; geobarometer; geothermometer; metapelite*

INTRODUCTION

Muscovite is ubiquitous in greenschist- to amphibolite-facies metapelites, thus making the garnet–muscovite (GM) geothermometer and the garnet–muscovite–plagioclase–quartz (GMPQ) geobarometer very important in determining the metamorphic *P–T* conditions of metapelitic rocks. For this reason, geothermometers and geobarometers applied to the pelitic mineral assemblage garnet + biotite + plagioclase + muscovite + quartz have been repeatedly calibrated (e.g. Krogh & Råheim, 1978; Ghent & Stout, 1981; Green & Hellman, 1982; Hodges & Crowley, 1985; Holdaway *et al.*, 1988; Hynes & Forest, 1988; Hoisch, 1990, 1991; McMullin *et al.*, 1991; Wu *et al.*, 2002, 2004*a*). In our earlier studies (Wu *et al.*, 2002, 2004*a*), the GM thermometer and

*Corresponding author. Telephone: +86-10-8825-6312. Fax: +86-10-8825-6012. E-mail: wucm@gucas.ac.cn

the GMPQ barometer are independent and were calibrated based on the garnet–biotite (GB) geothermometer (Holdaway, 2000; Model 5AV) and the GASP geobarometer (Holdaway, 2001). In this paper, we have refined these thermobarometers and made them thermodynamically interdependent, so that when biotite or aluminosilicate is absent in metapelites, the GM thermometer and the GMPQ barometer may provide reliable P–T estimates.

After extensive evaluation of the GB thermometers and the GASP barometers, Wu & Cheng (2006) concluded that the Holdaway (2000; Model 6AV) and the Kleemann & Reinhardt (1994) calibrations are the two most reliable GB thermometers. Each has small errors in reproducing the experimental temperatures and excellent accuracy in successfully discerning the systematic temperature changes of different metamorphic sequences, including prograde sequences, inverted metamorphic zones, and thermal contact aureoles. Further, it was concluded that the calibrations of Holdaway (2001) and Newton & Haselton [1981; based on Kleemann & Reinhardt's (1994) thermometer] are the most valid GASP barometers. In view of thermodynamic consistency, we prefer Holdaway's (2000; Model 6AV) GB thermometer and Holdaway's (2001) GASP barometer. Thus in this paper, input temperatures and pressures are simultaneously determined by these two thermobarometers.

THERMODYNAMIC BACKGROUND AND CALIBRATION

Thermodynamic models

The Fe and Mg exchange between coexisting garnet and muscovite can be described as (Krogh & Råheim, 1978; Green & Hellman, 1982; Hynes & Forest, 1988; Wu *et al.*, 2002)

$$\underset{\text{pyrope}}{Mg_3Al_2Si_3O_{12}} + \underset{\text{Fe-celadonite}}{3K(FeAl)Si_4O_{10}(OH)_2} = \underset{\text{almandine}}{Fe_3Al_2Si_3O_{12}} + \underset{\text{Mg-celadonite}}{3K(MgAl)Si_4O_{10}(OH)_2} \quad (1)$$

which constitutes the basis of the GM thermometer.

The GMPQ barometer is based on the following Mg- and Fe-endmember model equilibria (e.g. Hoisch, 1990, 1991; Wu *et al.*, 2004*a*):

$$\underset{\text{pyrope}}{Mg_3Al_2Si_3O_{12}} + \underset{\text{grossular}}{2Ca_3Al_2Si_3O_{12}} + \underset{\text{muscovite}}{3KAl_2(AlSi_3)O_{10}(OH)_2} + \underset{\text{quartz}}{6SiO_2} = \underset{\text{anorthite}}{6CaAl_2Si_2O_8} + \underset{\text{Mg-celadonite}}{3K(MgAl)Si_4O_{10}(OH)_2} \quad (2)$$

and

$$\underset{\text{almandine}}{Fe_3Al_2Si_3O_{12}} + \underset{\text{grossular}}{2Ca_3Al_2Si_3O_{12}} + \underset{\text{muscovite}}{3KAl_2(AlSi_3)O_{10}(OH)_2} + \underset{\text{quartz}}{6SiO_2} = \underset{\text{anorthite}}{6CaAl_2Si_2O_8} + \underset{\text{Fe-celadonite}}{3K(FeAl)Si_4O_{10}(OH)_2} \quad (3)$$

At equilibrium, when ignoring heat capacity, thermal expansion and compressibility of the phases involved, and assuming quartz to be a pure phase, the above three model reactions may be described respectively by the following three thermodynamic equations (Wu *et al.*, 2002; 2004*a*):

$$\begin{aligned} T(\mathrm{K}) = {} & (\Delta_1 H^0/\Delta_1 S^0) + [P(\mathrm{bars}) - 1]\cdot(\Delta_1 V^0/\Delta_1 S^0) \\ & + (W^{mus}_{FeMg}/\Delta_1 S^0)\cdot 3(X^{mus}_{Fe} - X^{mus}_{Mg}) \\ & + [(W^{mus}_{MgAl} - W^{mus}_{FeAl})/\Delta_1 S^0]\cdot 3X^{mus}_{Al} \\ & + (1/\Delta_1 S^0)\cdot[RT\ \ln\ K^{ideal}_{(1)} + (\mathrm{Fea} - \mathrm{Mga})\cdot T \\ & + (\mathrm{Feb} - \mathrm{Mgb})\cdot P + \mathrm{Fec} - \mathrm{Mgc}] \end{aligned} \quad (4)^{-1}$$

$$\begin{aligned} P_{(Mg)}(\mathrm{bars}) = {} & 1 - \Delta_2 H^0/\Delta_2 V^0 + T(\mathrm{K})(\Delta_2 S^0/\Delta_2 V^0) \\ & + (W^{mus}_{MgAl}/\Delta_2 V^0)\cdot 3(X^{mus}_{Mg} - X^{mus}_{Al}) \\ & + [(W^{mus}_{AlFe} - W^{mus}_{MgFe})/\Delta_2 V^0]\cdot 3X^{mus}_{Fe} \\ & + (1/\Delta_2 V^0)[T(\mathrm{K})(-R\ \ln\ K^{ideal}_{(2)} - 6\mathrm{Fa} \\ & + \mathrm{Mga} + 2\mathrm{Caa}) + P(-6\mathrm{Fb} + \mathrm{Mgb} + 2\mathrm{Cab}) \\ & - 6\mathrm{Fc} + \mathrm{Mgc} + 2\mathrm{Cac}] \end{aligned} \quad (5)$$

and

$$\begin{aligned} P_{(Fe)}(\mathrm{bars}) = {} & 1 - \Delta_3 H^0/\Delta_3 V^0 + T(\mathrm{K})(\Delta_3 S^0/\Delta_3 V^0) \\ & + (W^{mus}_{FeAl}/\Delta_3 V^0)\cdot 3(X^{mus}_{Fe} - X^{mus}_{Al}) \\ & + [(W^{mus}_{AlMg} - W^{mus}_{MgFe})/\Delta_3 V^0]\cdot 3X^{mus}_{Mg} \\ & + (1/\Delta_3 V^0)[T(\mathrm{K})(-R\ \ln\ K^{ideal}_{(3)} - 6\mathrm{Fa} \\ & + \mathrm{Fea} + 2\mathrm{Caa}) + P(-6\mathrm{Fb} + \mathrm{Feb} + 2\mathrm{Cab}) \\ & - 6\mathrm{Fc} + \mathrm{Fec} + 2\mathrm{Cac}] \end{aligned} \quad (6)$$

in which Caa, Cab, Cac, Fea, Feb, Fec, Mga, Mgb, Mgc, Fa, Fb and Fc are polynomial expressions describing the activity coefficients of garnet and plagioclase, consisting of the mole fractions of the endmembers of garnet and plagioclase and are described in the Appendix in Wu *et al.* (2004*b*). In the above three equations the subscripts 1, 2 and 3 refer to reactions (1), (2) and (3), respectively. ΔG is the Gibbs free energy of the respective

reaction at the P and T of interest. $K^{\text{ideal}}_{(1)}$, $K^{\text{ideal}}_{(2)}$ and $K^{\text{ideal}}_{(3)}$ are the respective equilibrium constants expressed as the products of ideal activities of the phases involved in each of the above reactions; these terms and the ideal activity models of the phases involved are defined in Table 1. In the equilibria expressions, ΔH^0, ΔS^0 and ΔV^0 refer to net changes in enthalpy, entropy and volume, respectively, of the given reaction involving pure phases at the standard state (298·15 K and 1 bar). It has been assumed that heat capacity, thermal expansion and compressibility of the reactions may be neglected, and this implies that ΔH^0, ΔS^0 and ΔV^0 do not vary or that any variation cancels out in the calibration range of pressure and temperature. For reactions involving only solid phases, this is a common and reasonable practice, which leads to negligible errors in P–T estimation.

To maintain thermodynamic consistency, we used the garnet activity model of Holdaway (2000, 2001). The activity coefficients of the grossular, pyrope and almandine phases in garnet, after rearrangement, may be written respectively as

$$RT\ \ln\ \gamma^{\text{grt}}_{\text{gros}} = 3RT\ \ln\ (\gamma^{\text{grt}}_{\text{Ca}}) = \text{Caa}\cdot T(\text{K}) + \text{Cab}\cdot P(\text{bars}) + \text{Cac} \quad (7)$$

$$RT\ \ln\ \gamma^{\text{grt}}_{\text{pyr}} = 3RT\ \ln\ (\gamma^{\text{grt}}_{\text{Mg}}) = \text{Mga}\cdot T(\text{K}) + \text{Mgb}\cdot P(\text{bars}) + \text{Mgc} \quad (8)$$

$$RT\ \ln\ \gamma^{\text{grt}}_{\text{alm}} = 3RT\ \ln\ (\gamma^{\text{grt}}_{\text{Fe}}) = \text{Fea}\cdot T(\text{K}) + \text{Feb}\cdot P(\text{bars}) + \text{Fec}. \quad (9)$$

Holdaway (2001) used the Al-avoidance plagioclase activity model of Fuhrman & Lindsley (1988). After rearranging, the expression of the activity coefficient of anorthite in plagioclase is expressed as

$$RT\ \ln\ (a^{\text{pl}}_{\text{an}}) = RT\ \ln\ [0{\cdot}25X^{\text{pl}}_{\text{Ca}}(1 + X^{\text{pl}}_{\text{Ca}})^2] + T(\text{K})\cdot\text{Fa} + P(\text{bars})\cdot\text{Fb} + \text{Fc}. \quad (10)$$

We have found that the mixing properties of muscovite solid solutions may be sufficiently described as symmetric Fe^{2+}–Mg–Al^{VI} ternary solutions, although much more complex activity models have been proposed (e.g. Coggon & Holland, 2002; Keller *et al.*, 2005).

Natural metapelitic samples

We have collated 103 natural metapelites containing the assemblage of garnet + biotite + muscovite + plagioclase + quartz + aluminosilicate(s) and these samples are listed in Electronic Appendix A. The selection criteria of samples have been given by Hoisch (1990, 1991). Furthermore, plagioclase should be free of chemical zoning (R. Offler, personal communication, 2005). These samples fall in the mineral composition ranges: $X^{\text{grt}}_{\text{Fe}}$ = 0·53–0·81, $X^{\text{grt}}_{\text{Mg}}$ = 0·05–0·24 and $X^{\text{grt}}_{\text{Ca}}$ = 0·03–0·23 in garnet, and $X^{\text{pl}}_{\text{Ca}}$ = 0·17–0·74 in plagioclase. For muscovite, the chemical compositions are restricted to Fe = 0·04–0·16, Mg = 0·04–0·13 and Al^{VI} = 1·74–1·96, on the basis of 11 oxygens in muscovite. Samples with $X^{\text{grt}}_{\text{Ca}} < 0{\cdot}03$ or $X^{\text{pl}}_{\text{Ca}} < 0{\cdot}17$ have been omitted because of the calcium-deficient effect, which may lead to larger errors in pressure estimates (Todd, 1998; Holdaway, 2001). The P–T ranges of these samples are 0·8–11·1 kbar and 452–758°C, determined simultaneously by the GB thermometer (Holdaway, 2000) and the GASP barometer (Holdaway, 2001).

Of these samples, eight contain andalusite, 26 contain sillimanite, 56 contain kyanite, four contain andalusite + sillimanite, and nine contain sillimanite + kyanite. Ferric iron in garnet is assumed to be 3% of the total iron. For biotite, 11·6% ferric iron is assumed for the graphite–ilmenite-bearing samples, and 20% for the magnetite-bearing samples. This treatment is identical to that of Holdaway (2000, 2001), to maintain thermodynamic consistency in using the GB and GASP thermobarometer (Holdaway, 2000, 2001). Ferric iron contents in muscovite are difficult to estimate, so we assumed two cases: Model A, assuming no ferric iron in muscovite; Model B, assuming 50% ferric iron in muscovite.

Table 1: Ideal activities of the mineral phases and equilibrium constants of the model reactions

Garnet

$X^{\text{grt}}_{\text{alm}} = (X^{\text{grt}}_{\text{Fe}})^3$, $X^{\text{grt}}_{\text{pyr}} = (X^{\text{grt}}_{\text{Mg}})^3$, $X^{\text{grt}}_{\text{gros}} = (X^{\text{grt}}_{\text{Ca}})^3$, $X^{\text{grt}}_{\text{sps}} = (X^{\text{grt}}_{\text{Mn}})^3$

$X^{\text{grt}}_{\text{Fe}} = \text{Fe}^{2+}/(\text{Fe}^{2+} + \text{Mg} + \text{Ca} + \text{Mn})$, $X^{\text{grt}}_{\text{Mg}} = \text{Mg}/(\text{Fe}^{2+} + \text{Mg} + \text{Ca} + \text{Mn})$

$X^{\text{grt}}_{\text{Ca}} = \text{Ca}/(\text{Fe}^{2+} + \text{Mg} + \text{Ca} + \text{Mn})$, $X^{\text{grt}}_{\text{Mn}} = \text{Mn}/(\text{Fe}^{2+} + \text{Mg} + \text{Ca} + \text{Mn})$

Muscovite

$X^{\text{mus}}_{\text{mus}} = (X^{\text{mus}}_{\text{Al}})^2$, $X^{\text{mus}}_{\text{Mg-cel}} = 4(X^{\text{mus}}_{\text{Mg}})(X^{\text{mus}}_{\text{Al}})$, $X^{\text{mus}}_{\text{Fe-cel}} = 4(X^{\text{mus}}_{\text{Fe}})(X^{\text{mus}}_{\text{Al}})$

$X^{\text{mus}}_{\text{Fe}} = \text{Fe}^{2+}/(\text{Fe}^{2+} + \text{Mg} + \text{Al}^{\text{VI}})$, $X^{\text{mus}}_{\text{Mg}} = \text{Mg}/(\text{Fe}^{2+} + \text{Mg} + \text{Al}^{\text{VI}})$

$X^{\text{mus}}_{\text{Al}} = \text{Al}^{\text{VI}}/(\text{Fe}^{2+} + \text{Mg} + \text{Al}^{\text{VI}})$

Plagioclase

$X^{\text{pl}}_{\text{an}} = \frac{1}{4}X^{\text{pl}}_{\text{Ca}}(1 + X_{\text{Ca}})^2$, $X^{\text{pl}}_{\text{ab}} = X^{\text{pl}}_{\text{Na}}$, $X^{\text{pl}}_{\text{or}} = X^{\text{pl}}_{\text{K}}$

$X^{\text{pl}}_{\text{Ca}} = \text{Ca}/(\text{Ca} + \text{Na} + \text{K})$, $X^{\text{pl}}_{\text{Na}} = \text{Na}/(\text{Ca} + \text{Na} + \text{K})$

$X^{\text{pl}}_{\text{K}} = \text{K}/(\text{Ca} + \text{Na} + \text{K})$

Equilibrium constants

$$K^{\text{ideal}}_{(1)} = \frac{(X^{\text{grt}}_{\text{alm}})(X^{\text{mus}}_{\text{Mg-cel}})^3}{(X^{\text{grt}}_{\text{pyr}})(X^{\text{mus}}_{\text{Fe-cel}})^3} = \frac{(X^{\text{grt}}_{\text{Fe}})^3(X^{\text{mus}}_{\text{Mg}})^3}{(X^{\text{grt}}_{\text{Mg}})^3(X^{\text{mus}}_{\text{Fe}})^3}$$

$$K^{\text{ideal}}_{(2)} = \frac{(X^{\text{pl}}_{\text{an}})^6(X^{\text{mus}}_{\text{Mg-cel}})^3}{(X^{\text{grt}}_{\text{pyr}})(X^{\text{grt}}_{\text{gros}})^2(X^{\text{mus}}_{\text{mus}})^3(X^{\text{qtz}}_{\text{qtz}})^6} = \frac{(X^{\text{pl}}_{\text{Ca}})^6(1 + X^{\text{pl}}_{\text{Ca}})^{12}(X^{\text{mus}}_{\text{Mg}})^3}{64{\cdot}0(X^{\text{grt}}_{\text{Mg}})^3(X^{\text{grt}}_{\text{Ca}})^6(X^{\text{mus}}_{\text{Al}})^3}$$

$$K^{\text{ideal}}_{(3)} = \frac{(X^{\text{pl}}_{\text{an}})^6(X^{\text{mus}}_{\text{Fe-cel}})^3}{(X^{\text{grt}}_{\text{alm}})(X^{\text{grt}}_{\text{gros}})^2(X^{\text{mus}}_{\text{mus}})^3(X^{\text{qtz}}_{\text{qtz}})^6} = \frac{(X^{\text{pl}}_{\text{Ca}})^6(1 + X^{\text{pl}}_{\text{Ca}})^{12}(X^{\text{mus}}_{\text{Fe}})^3}{64{\cdot}0(X^{\text{grt}}_{\text{Fe}})^3(X^{\text{grt}}_{\text{Ca}})^6(X^{\text{mus}}_{\text{Al}})^3}$$

Calibration

The mineral composition and P–T data from the metapelitic samples in Electronic Appendix A were

Table 2: Regression summary (±2σ)

(a) The garnet–muscovite (GM) geothermometry

	Δ_1H^0/Δ_1S^0 (K)	Δ_1V^0/Δ_1S^0 (K/bar)	$W^{mus}_{FeMg}/\Delta_1S^0$ (K)	$(W^{mus}_{MgAl}-W^{mus}_{FeAl})/\Delta_1S^0$ (K)	$1/\Delta_1S^0$ (K/J)	R
Model A	2325·8 (±162·0)	−0·0001 (±0·001)	−2180·4 (±99·3)	−375·9 (±63·4)	−0·0135 (±0·001)	0·920
Model B	2064·7 (±380·4)	−0·0007 (±0·001)	−2359·3 (±239·7)	−313·9 (±147·0)	−0·0098 (±0·001)	0·876

(b) The garnet–muscovite–plagioclase–quartz (GMPQ) geobarometry

Model	Δ_2H^0/Δ_2V^0 (bar)	Δ_2S^0/Δ_2V^0 (bar/K)	$W^{mus}_{MgAl}/\Delta_2V^0$ (bar)	$(W^{mus}_{AlFe}-W^{mus}_{MgFe})/\Delta_2V^0$ (bar)	$1/\Delta_2V^0$ (bar/J)	R
P(2A)	−13417·8 (±1301·3)	17·735 (±0·4)	5999·7 (±391·9)	−7933·4 (±646·5)	0·083 (±0·001)	0·996
P(2B)	−13255·4 (±1280·9)	17·690 (±0·4)	5930·3 (±384·2)	−10016·8 (±1019·4)	0·083 (±0·001)	0·996
Model	Δ_3H^0/Δ_3V^0 (bar)	Δ_3S^0/Δ_3V^0 (bar/K)	$W^{mus}_{FeAl}/\Delta_3V^0$ (bar)	$(W^{mus}_{AlMg}-W^{mus}_{MgFe})/\Delta_3V^0$ (bar)	$1/\Delta_3V^0$ (bar/J)	R
P(3A)	−7096·2 (±606·3)	20·510 (±0·3)	5721·9 (±193·1)	−3436·1 (±669·6)	0·083 (±0·0006)	0·998
P(3B)	−22396·1 (±1113·1)	19·044 (±0·3)	10802·6 (±369·9)	−8439·5 (±776·8)	0·083 (±0·001)	0·998

inserted into equations (4)–(6), and these over-determined temperature- and pressure-dependent equations were subjected to nonlinear multiple regression analyses to obtain unknown parameters that minimized the sum of squares of residuals in temperature or pressure. Through non-linear iterative regressions for the thermobarometer equations, the unknowns in equations (4)–(6) have been obtained and are listed in Table 2. It should be noted that the thermodynamic parameters derived in this paper are just ratios of thermodynamic parameters, so they cannot be compared with the predicted thermodynamic parameters from any thermodynamic dataset.

The regressions have been weighted. We have multiplied the numbers of the low- and high-temperature samples (i.e. low- and high-temperature samples participated in the regressions several times), so that temperatures of the calibration samples are nearly equally distributed. The same is done for the low- and high-pressure samples. This method is statistically valid and has greatly improved the regression quality.

Inserting the regressed thermodynamic parameters (Table 2) into equation (4) gives two new formulations of the GM geothermometer:

(a) Model A, assuming no ferric iron in muscovite

$$T_{(a)}(\mathrm{K}) = \{2325{\cdot}8 + P(\mathrm{kbar})[-0{\cdot}1 - 13{\cdot}5(\mathrm{Feb}-\mathrm{Mgb})] - 0{\cdot}0135(\mathrm{Fec}-\mathrm{Mgc}) - 6541{\cdot}2(X^{mus}_{Fe}-X^{mus}_{Mg}) - 1127{\cdot}7X^{mus}_{Al}\}/\{1 + 0{\cdot}0135[R\ \ln K^{ideal}_{(1)} + (\mathrm{Fea}-\mathrm{Mga})]\} \quad (11a)$$

and

(b) Model B, assuming 50% Fe^{3+} contents in muscovite

$$T_{(b)}(\mathrm{K}) = \{2064{\cdot}7 + P(\mathrm{kbar})[-0{\cdot}7 - 9{\cdot}8(\mathrm{Feb}-\mathrm{Mgb})] - 0{\cdot}0098(\mathrm{Fec}-\mathrm{Mgc}) - 7077{\cdot}9(X^{mus}_{Fe}-X^{mus}_{Mg}) - 941{\cdot}7X^{mus}_{Al}\}/\{1 + 0{\cdot}0098[R\ \ln K^{ideal}_{(1)} + (\mathrm{Fea}-\mathrm{Mga})]\} \quad (11b)$$

as well as four GMPQ geobarometer formulae from equations (5) and (6) as follows:

(c) Mg model GMPQ barometer $P_{(Mg\,a)}$, assuming 0% Fe^{3+} in muscovite

$$P_{(Mg\,a)}(\mathrm{bars}) = \{13418{\cdot}8 + 17{\cdot}735T(\mathrm{K}) + 17999{\cdot}1(X^{mus}_{Mg}-X^{mus}_{Al}) - 23800{\cdot}2X^{mus}_{Fe} + 0{\cdot}083[T(\mathrm{K})(-R\ln K^{ideal}_{(2)} - 6\mathrm{Fa} + \mathrm{Mga} + 2\mathrm{Caa}) - 6\mathrm{Fc} + \mathrm{Mgc} + 2\mathrm{Cac}]\}/[1 - 0{\cdot}083(-6\mathrm{Fb} + \mathrm{Mgb} + 2\mathrm{Cab})] \quad (12a)$$

(d) Mg model GMPQ barometer $P_{(Mg\,b)}$, assuming 50% Fe^{3+} in muscovite

$$P_{(Mg\,b)}(\mathrm{bars}) = \{13256{\cdot}4 + 17{\cdot}690T(\mathrm{K}) + 17790{\cdot}9(X^{mus}_{Mg}-X^{mus}_{Al}) - 30050{\cdot}4X^{mus}_{Fe} + 0{\cdot}083[T(\mathrm{K})(-R\ln K^{ideal}_{(2)} - 6\mathrm{Fa} + \mathrm{Mga} + 2\mathrm{Caa}) - 6\mathrm{Fc} + \mathrm{Mgc} + 2\mathrm{Cac}]\}/[1 - 0{\cdot}083(-6\mathrm{Fb} + \mathrm{Mgb} + 2\mathrm{Cab})] \quad (12b)$$

(e) Fe model GMPQ barometer $P_{(\mathrm{Fe\,a})}$, assuming 0% Fe^{3+} in muscovite

$$P_{(\mathrm{Fe\,a})}(\mathrm{bars}) = \{7097{\cdot}2 + 20{\cdot}510T(\mathrm{K}) + 17165{\cdot}7(X_{\mathrm{Fe}}^{\mathrm{mus}} - X_{\mathrm{Al}}^{\mathrm{mus}}) - 10308{\cdot}3X_{\mathrm{Mg}}^{\mathrm{mus}} + 0{\cdot}083[T(\mathrm{K})(-R\ln K_{(3)}^{\mathrm{ideal}} - 6\mathrm{Fa} + \mathrm{Fea} + 2\mathrm{Caa}) - 6\mathrm{Fc} + \mathrm{Fec} + 2\mathrm{Cac}]\}/[1 - 0{\cdot}083(-6\mathrm{Fb} + \mathrm{Feb} + 2\mathrm{Cab})] \quad (12c)$$

and

(f) Fe model GMPQ barometer $P_{(\mathrm{Fe\,b})}$, assuming 50% Fe^{3+} in muscovite

$$P_{(\mathrm{Fe\,b})}(\mathrm{bars}) = \{22397{\cdot}1 + 19{\cdot}044T(\mathrm{K}) + 32407{\cdot}8(X_{\mathrm{Fe}}^{\mathrm{mus}} - X_{\mathrm{Al}}^{\mathrm{mus}}) - 25318{\cdot}5X_{\mathrm{Mg}}^{\mathrm{mus}} + 0{\cdot}083[T(\mathrm{K})(-R\ln K_{(3)}^{\mathrm{ideal}} - 6\mathrm{Fa} + \mathrm{Fea} + 2\mathrm{Caa}) - 6\mathrm{Fc} + \mathrm{Fec} + 2\mathrm{Cac}]\}/[1 - 0{\cdot}083(-6\mathrm{Fb} + \mathrm{Feb} + 2\mathrm{Cab})]. \quad (12d)$$

The resulting GM thermometers (Models A and B) generally reproduced the GB temperatures within ±50°C (Electronic Appendix A, Fig. 1a and b). The two GM thermometer formulations gave identical temperatures well within ±40°C for every sample (Electronic Appendix A, Fig. 1c). The resulting four formulations of the GMPQ barometer generally reproduced the GASP pressures within ±1·0 kbar (Electronic Appendix A, Fig. 2a and b; Models A and B). We have found that Model A and Model B formulations of the Mg-endmember GMPQ barometer gave identical pressure estimates well within ±0·5 kbar for every sample (Electronic Appendix A). Such a comparison is based on simultaneously applying the GM–GMPQ thermobarometer Model A and Model B, respectively. When the input temperature is the same value, the pressure difference of the Mg-endmember GMPQ barometer using the different models is reduced to ±15 bars. Similar results come from the Fe-model GMPQ barometer (Electronic Appendix A). Furthermore, the Mg-model and Fe-model GMPQ barometers gave similar pressure estimates well within ±0·5 kbar for every sample (Electronic Appendix A, Fig. 2c).

APPLICATIONS OF THE GM GEOTHERMOMETER AND THE GMPQ GEOBAROMETER

To test the applicability of the GM thermometer and the GMPQ barometer, we have applied these formulae [equations (11a), (11b) and (12a)–(12d)] to natural metapelitic rocks (Electronic Appendix B) not included in

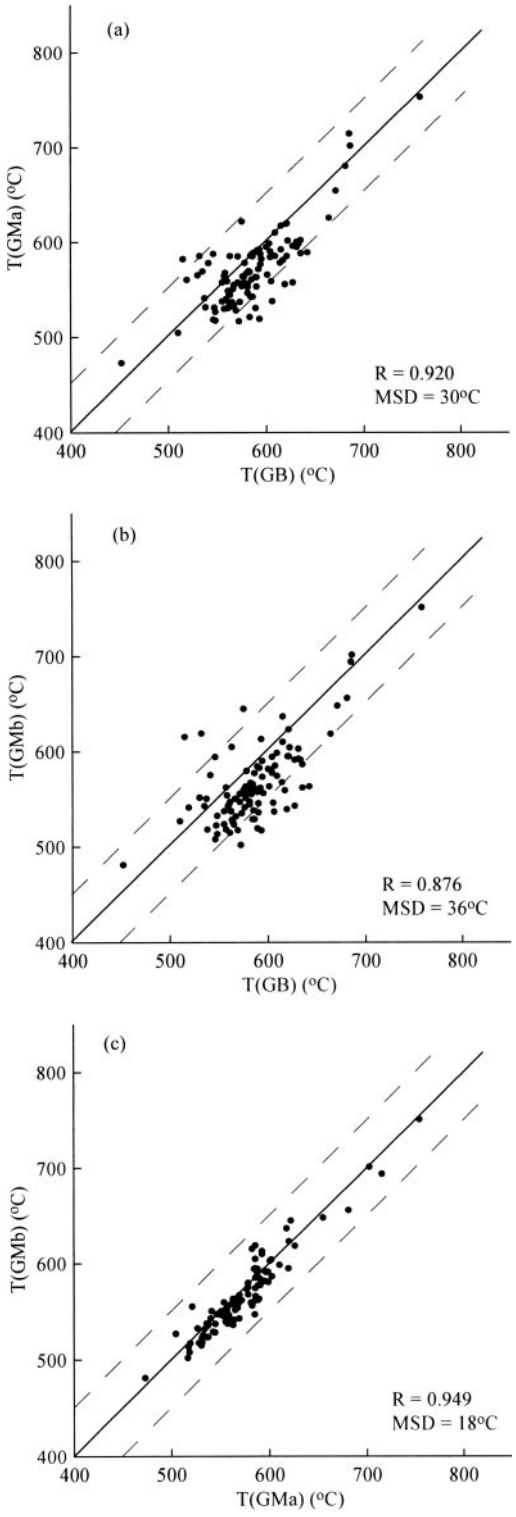

Fig. 1. Relationships between the temperatures calculated using the GM and GB thermometers. Continuous line represents 1:1 correlation. Dashed lines represent ±50°C deviation. (a) GB temperatures vs GM temperatures (Model A); (b) GB temperatures vs GM temperatures (Model B); (c) GM temperatures (Model A) vs GM temperatures (Model B).

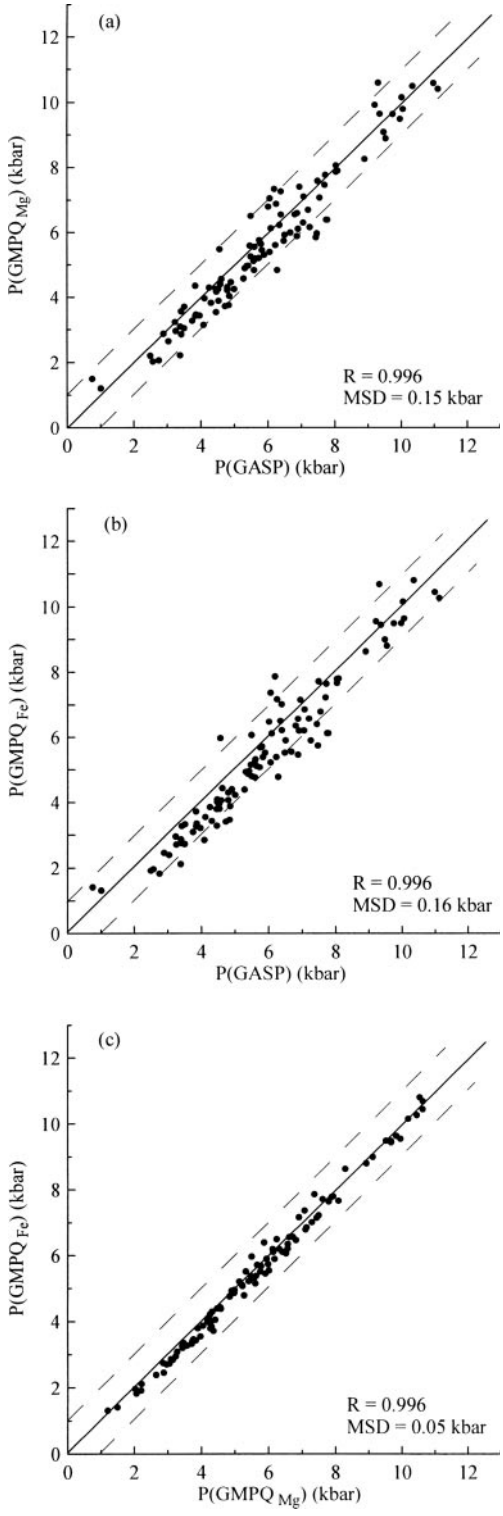

Fig. 2. Relationships between pressures calculated using the GMPQ and GASP barometers. Continuous line represents 1:1 correlation. Dashed lines represent ±1·0 kbar deviation. (a) GASP pressures vs GMPQ pressures (Model A); (b) GASP pressures vs GMPQ pressures (Model B); (c) GMPQ pressures (Model A) vs GMPQ pressures (Model B).

calibrating the thermobarometer. When possible, we simultaneously applied the GM thermometer and GMPQ barometer (see Fig. 3). When plagioclase is absent, or calcium content in garnet or plagioclase is deficient and thus the GMPQ barometer cannot be used, we applied the GM thermometer based on assumed pressures according to the estimated pressures in the literature or from comparison with the GASP pressures of nearby samples. Although there are uncertainties in the assumed pressures, we believe that such errors may not translate to meaningful GM temperature errors because the GM thermometer is fairly little pressure-dependent.

Application of the GM geothermometer

To test its applicability, the GM thermometer has been applied to rocks of prograde sequences, an inverted metamorphic zone and thermal contact aureoles.

In the Snow Peak area, northern Idaho, USA, Barrovian-type metamorphic sequences have been found in the metapelites (Lang & Rice, 1985). From NE to SW, the metamorphic grade progressively changes from low to high grades with chlorite–biotite, garnet, staurolite, transition, staurolite–kyanite and kyanite zones appearing in sequence. These zones were metamorphosed in a second metamorphic event M_2 and the mineral assemblages are post-kinematic. Both the GB and GM thermometer successfully reflect the expected systematic temperature change, although the GM thermometer yielded a steeper thermal gradient than that of the GB thermometer (Electronic Appendix B, Fig. 4a). This is partly because the GM thermometer is slightly less pressure-dependent than the GB thermometer (see Fig. 3), so the GM temperatures are less influenced by the pressure values. The GM thermometer using Model A shows nearly identical results to Model B, except that Model B yields indistinguishable temperatures for the chlorite–biotite zone and garnet zone, similar to the GB thermometer (Fig. 4a).

In the central Menderes Massif, Turkey, an orderly prograde metamorphic zonation appears sequentially as garnet, staurolite, staurolite–kyanite and kyanite zones (Ashworth & Evirgen, 1985*a*, 1985*b*). No muscovite is found in the kyanite zone samples. In the application of the GM thermometer, chemical compositions of the muscovite in the garnet zone (sample A181.1), the staurolite zone (sample 858C) and the staurolite–kyanite zone (sample A40) exceed the calibration range and thus these samples have been excluded. Both the GB and GM thermometer (Model A) reflect the expected systematic temperature change, with the GM thermometer yielding a slightly steeper thermal gradient (Electronic Appendix B, Fig. 4b). However, GM thermometer (Model B) shows a lower temperature for the

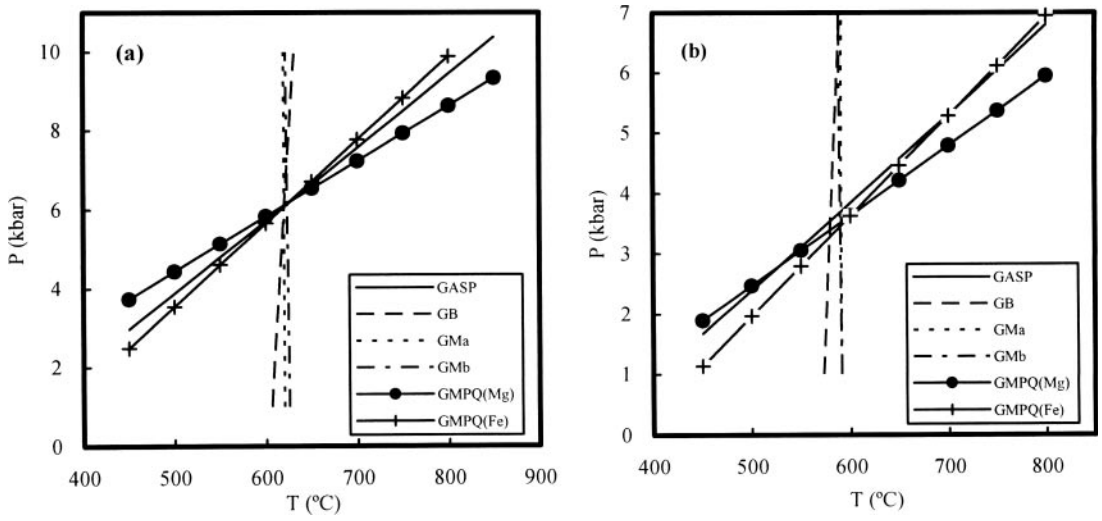

Fig. 3. Simultaneous application of the GM thermometer and the GMPQ barometer. (a) kyanite-bearing sample Mag310 (Engi *et al.*, 1995) was included in the calibration; (b) sillimanite-bearing sample 2040-2 (Gordon *et al.*, 1991) was not included in the calibration.

staurolite–kyanite zone than that of the staurolite zone, which is not the case.

An inverted metamorphic gradient is preserved in the western metamorphic belt near Juneau, Alaska, USA. Thermal peak metamorphic conditions were seen to increase structurally upward over a distance of about 8 km (Himmelberg *et al.*, 1991). The chemical composition of the garnet zone sample (20B) exceeds the calibration range and thus has been excluded. Both the GM (Model A) and the GB thermometers indicate similar temperatures increasing progressively from the garnet zone to the staurolite–biotite, lower kyanite–biotite, higher kyanite–biotite and sillimanite zones (Electronic Appendix B, Fig. 4c). Model B of the GM thermometer yields unreasonably high temperature for the staurolite–biotite zone.

Metamorphism around syntectonic granitoids in the Eastern Rouergue, France, produced a thermal contact aureole with progressively developed metamorphic zones of chlorite, biotite, garnet, staurolite and kyanite (Delor *et al.*, 1984). No garnet is found in the chlorite and biotite zones. One kyanite zone sample (153) has no muscovite. All of the other samples show the expected systematic temperature changes through the different zones, using both the GM and GB thermometers (Electronic Appendix B, Fig. 4d). It is noted that the GB temperatures are higher than the GM temperatures by about 10–70°C.

Five regional contact metamorphic events (M_1–M_5) occurred in west–central Maine in the Devonian and Carboniferous, among which the M_3 and M_5 events are the two most important metamorphic events (Holdaway *et al.*, 1988). Each metamorphic event is closely associated with emplacement of S-type granites, such that the isograd patterns produced in the surrounding pelitic schists generally mirror the geometry of plutonic intrusive contacts. From north to south the metamorphic grade varies from chlorite to sillimanite, K-feldspar and muscovite, and these zones are designated from low to high grades as Grades 3, 4, 5, 6 (M_3) and Grades 6·5, 7 and 8 (M_5), respectively (Holdaway *et al.*, 1988). The chemical compositions of muscovite in the Grade 4 samples (27, 52 and 114) and in the Grade 6 sample (79) exceed the calibration range and thus these samples were excluded. Both the GM and the GB thermometers yield the expected systematic temperature changes through the progressive metamorphic grades (Electronic Appendix B, Fig. 4e).

From the above application it is suggested that the GM thermometer calibrated in this work, particularly Model A, may be used as a practical and reasonable tool in deciphering the metamorphic temperatures of metapelites.

Application of the GMPQ geobarometer

Simultaneously applying the GM thermometer and the GMPQ barometer to the aluminosilicate-bearing samples, yielded reasonable *P–T* estimates (Electronic Appendix B), and generally put the samples into the appropriate aluminosilicate stability field or near the phase transition boundaries (Fig. 5a–c). However, several samples were placed in the incorrect aluminosilicate stability fields using the Model B results of the GM–GMPQ thermobarometer.

It is accepted that rocks formed at thermodynamic equilibrium within a limited contact aureole should have been metamorphosed at the same pressure

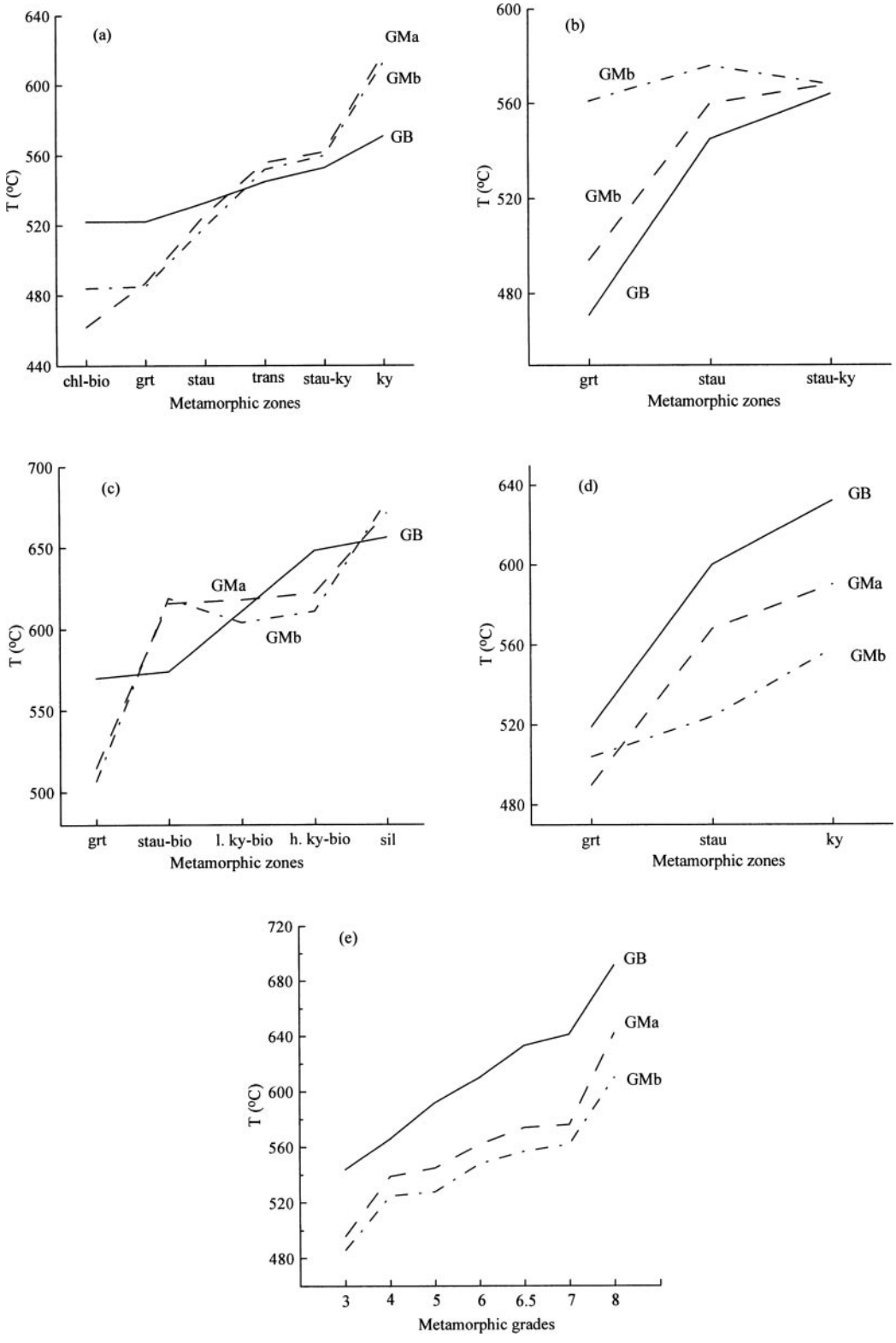

Fig. 4. Application of the GM thermometer to different metamorphic zones. (a) The northern Idaho Barrovian series sequences, USA (Lang & Rice, 1985); (b) the prograde sequences in the central Menderes, Turkey (Ashworth & Evirgen, 1985*a*, 1985*b*); (c) the Juneau inverted zones near Juneau, Alaska, USA (Himmelberg *et al.*, 1991); (d) the contact zones in Eastern Rouergue, France (Delor *et al.*, 1984); (e) the regional contact zones in west–central Maine, USA (Holdaway *et al.*, 1988).

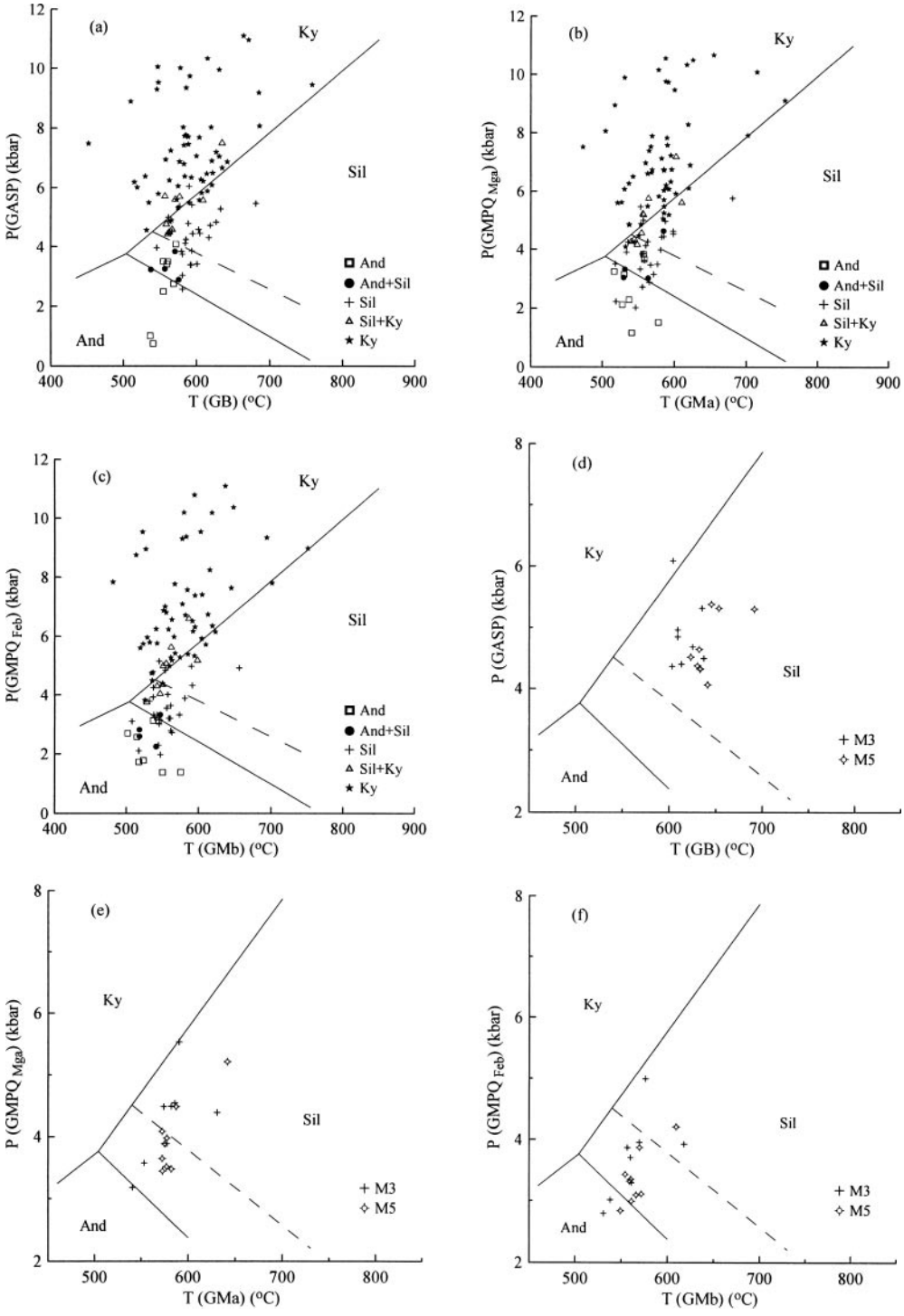

Fig. 5. (a–c) *P–T* plot of the aluminosilicate-bearing pelitic samples used in calibrating the GM thermometer and the GMPQ barometer (Electronic Appendix A). (d–f) *P–T* plot of the sillimanite-bearing metapelites of the regional contact zones, west–central Maine, USA (Holdaway *et al.*, 1988) not used in calibrating the GM thermometer and the GMPQ barometer. (a) and (d) show pressures and temperatures determined by the GB thermometer (Holdaway, 2000) and the GASP barometer (Holdaway, 2001); (b) and (e) show pressures and temperatures determined by the GM thermometer (Model A) and the GMPQ barometer (Mg-endmember model reaction, Model A); (c) and (f) show pressures and temperatures determined by the GM thermometer (Model B) and the GMPQ barometer (Fe-endmember model reaction, Model B). The crosses stand for the M_3 assemblages, and the crosses with circles stand for the M_5 assemblages (Holdaway *et al.*, 1988). Continuous lines represent the aluminosilicate equilibria of Holdaway *et al.* (1998). Dashed line represents the andalusite = sillimanite equilibrium of Pattison (1992).

(Wu & Cheng, 2006). Thus the applicability of the GMPQ barometer can be checked by applying it to contact aureole rocks.

A good example again occurs in the west–central Maine where regional contact metamorphic zones cover a large area. Although Holdaway *et al.* (1988) suggested that M_3 occurred at 3·1 kbar and M_5 at 3·8 kbar, various GASP barometers show no obvious pressure difference more than 0·5 kbar between M_3 and M_5 rocks and thus they can be regarded as identical, within error (Wu & Cheng, 2006). The GASP barometer (Holdaway, 2001) shows that M_3 occurred at 4·9 kbar and M_5 occurred at 4·7 kbar, respectively (Electronic Appendix B). The GMPQ barometer, however, yielded M_3 at 4·1 kbar (Mg-endmember barometer) or 3·8 kbar (Fe-endmember barometer), and M_5 at 3·9 kbar (Mg-endmember barometer) or 3·5 kbar (Fe-endmember barometer), respectively, also identical to the GASP barometer, within error (Electronic Appendix B). These pressure determinations are depicted in Fig. 5d–f. In the pressure determination, the samples devoid of plagioclase were excluded. In our computation, chemical compositions of muscovite in the Grade 4 samples (27, 52 and 114) as well as the Grade 6 sample (79) exceed the calibration range, so these samples were excluded. Also excluded are the calcium-deficient samples, including the Grade 6 sample (19), and the Grade 6·5 sample (91) as well as the Grade 7 sample (86).

In general, rocks within a very limited area that have not been disrupted by later deformation events should show no obvious pressure variation, and this phenomenon is an independent criterion in testing the applicability of a barometer (Wu & Cheng, 2006).

Gordon *et al.* (1991) collected six metapelitic samples within 800 m of each other that straddle the sillimanite–biotite isograd in the File Lake area, Manitoba, Canada (Electronic Appendix B). Among these, sample 20-27 contains sillimanite but not garnet, sample 2026-2 contains no muscovite, samples 2026-2 and 2040-2 contain sillimanite, and the other three samples (1001, 2025A and 2038) contain garnet but no aluminosilicate. The GB thermometer and GASP barometer yielded P–T conditions of 556°C and 3·6 kbar and 594°C and 3·8 kbar for the sillimanite-bearing samples 2026-2 and 2040-2, respectively. Therefore it is reasonable to infer that the rocks were metamorphosed at *c.* 3·7 kbar (Wu & Cheng, 2006). Simultaneously applying the GM thermometer and the GMPQ barometer to the metapelites yielded temperatures of 525–538°C and pressures of 2·5–2·6 kbar for the three aluminosilicate-absent samples, and 604°C and 3·7 kbar for the sillimanite-bearing sample 2040-2. The GMPQ barometer yielded an averaged pressure of 2·9 ± 0·5 kbar, close to the assumed constant pressure of 3·7 kbar, within error (Electronic Appendix B).

The closely associated aluminosilicate-absent sample SWW-20b and the sillimanite-bearing sample SWW-9 in the contact aureole, central Old Woman Mountains, southeastern California (Rothstein & Hoisch, 1994), were metamorphosed at 621–657°C and 3·5 kbar, determined by GB and GASP thermobarometer simultaneously. Simultaneously applying the GM thermometer and GMPQ barometer yielded metamorphic temperature of 568–583°C and pressure of 2·1–2·5 kbar for the aluminosilicate-free sample SWW-20b, identical within error to that of the sillimanite-bearing sample SWW-9, 586–605°C and 2·7–3·3 kbar, respectively (Electronic Appendix B).

Application of the GM–GMPQ thermobarometer to the three regions (Holdaway *et al.*, 1988; Gordon *et al.*, 1991; Rothstein & Hoisch, 1994) yielded *c.* 1 kbar lower GMPQ pressures than GASP pressures for most of the investigated samples. This is an artifact because we occasionally obtained relatively lower GM temperatures than GB temperatures for these samples, which in turn translated to lower GMPQ pressures. This does not suggest that the GMPQ barometer gives systematically lower pressures than the GASP barometer. When input temperatures are the same as that in applying the GASP barometer, the GMPQ pressures obtained are similar to that of GASP.

Application of the GMPQ barometer suggests that this barometer may be useful in determining metamorphic pressures, when considering the concordance between the GASP and GMPQ pressures, and the reasonable pressure estimates.

ERROR CONSIDERATIONS

Errors in a geothermometer or a geobarometer come from the input pressure or input temperature, errors on the uncertainties of activity models, and analytical uncertainties of the chemical compositions of minerals. Combined, these errors may propagate to a somewhat large total uncertainty for T and P values calculated using a geothermometer or a geobarometer. However, the total error of the GM thermometer or the GMPQ barometer is difficult to determine through the error propagation method (e.g. Spear, 1995) because of the complexity of the activity models of the mineral phases.

By analogy with the GB thermometer, which is experimentally calibrated, the absolute error of the GM thermometer may be expected to be *c.* 70°C (see Fig. 1), although no experiments have been performed to calibrate the GM thermometer. Random errors in this thermometer come from the error in pressure estimates and analytical errors of garnet and muscovite. For our collated samples, pressure errors of ±2·0 kbar may propagate to an estimated temperature error of less than ±1·1°C for both Models A and B; that is, nearly

independent of pressure and much lower than that of the GB thermometer. Through numerical simulation of the calibration samples (Electronic Appendix A) we have found that an analytical error of ±2% of Fe or Mg in muscovite, or Fe or Mg in garnet, may introduce temperature errors of ±1·9–2·4°C, ±0·8–1·9°C, ±1·0–5·9°C and ±1·0–5·2°C for Model A, and ±0·6–1·9°C, ±0·5–3°C, ±2·2–3·9°C and ±1·9–3·4°C for Model B, respectively. We may, therefore, expect that the total random error of the GM thermometer will be be no more than ±16°C.

Because of the lack of experimental GMPQ calibrations, the absolute errors of the GMPQ barometer formulae cannot be evaluated. However, the very close correlation between the GASP and GMPQ barometers (Fig. 2) suggests that the GMPQ barometer is in excellent accord with the GASP barometer within ±1·4 kbar (mostly within ±0·5 kbar) in the wide P–T range of 1·0–11·1 kbar and 450–750°C.

Numerical simulation of the calibration samples (Electronic Appendix A) shows that an analytical error of ±2% of Fe, Mg and Al^{VI} in muscovite, and Fe, Mg and Ca in garnet, and Ca in plagioclase, may introduce pressure errors of ±3–25 bars, ±3–23 bars, ±1–25 bars, ±21–97 bars, ±4–28 bars, ±44–79 bars and ±6–84 bars, respectively. A temperature error of ±50°C will introduce a pressure error of ±509–1451 bars. Therefore we may expect that the random error of the GMPQ geobarometer will be around ±1·5 kbar.

DISCUSSION

It is found that the differences between the GM and GB temperatures are independent of the celadonite content of muscovite (Electronic Appendix C). Similarly, the differences between the GMPQ and GASP pressures are independent of the calcium content of plagioclase, or calcium content of garnet, or celadonite contents of muscovite, as indicated in Electronic Appendix D. However, we have found that the pressure difference between the Mg- and Fe-endmember GMPQ barometer is slightly linearly correlated with the celadonite content of muscovite. This is possibly because Model B assumes 50% total Fe as ferric in muscovite; thus ferrous Fe is more diluted for Model B and smaller analytical error of muscovite may possibly translate to larger GMPQ pressure errors, so the pressure difference between Model A and Model B possibly becomes larger for the Mg-rich muscovites. We thus do not advocate application of the GM thermometer and the GMPQ barometer to metapelitic rocks with muscovite of Mg >0·13 or Fe <0·04 atoms on the basis of 11 oxygens.

The P/T slope of the GM thermometer is steeper than that of the GB thermometer (see Fig. 3); that is, the GM thermometer is less pressure dependent than the GB thermometer. However, the P/T slopes of the GMPQ and GASP barometers are nearly identical (see Fig. 3).

The new GM thermometer and GMPQ barometer may be simultaneously applied to metapelites in determining metamorphic P–T conditions, especially when biotite or aluminosilicate is absent. When biotite and aluminosilicate(s) are present, the GB thermometer (Holdaway, 2000; Model 6AV) and the GASP barometer (Holdaway, 2001) are preferable because they have been calibrated using experimental data and confirmed by natural data and have been found to be the most valid among the various versions of such thermobarometers (Wu & Cheng, 2006).

A GM–GMPQ thermobarometer program is available as an EXCEL spreadsheet in the electronic supplementary material at the journal's website. This is also available from the authors.

ACKNOWLEDGEMENTS

Reviews by Robin Offler, Nathan R. Daczko and Julie Hollis, and the editorial review by Geoffrey Clarke have substantially improved the quality of the original manuscript. This research was supported by the National Natural Science Foundation of China (40472045, 40429001) and the Hong Kong Research Grants Council (7055/03P, 7058/04P, 7055/05P). This paper is in honour of Ms Bani Zhang.

SUPPLEMENTARY DATA

Supplementary data for this paper are available on *Journal of Petrology* online.

REFERENCES

Ashworth, J. R. & Evirgen, M. M. (1985a). Plagioclase relations in pelites, central Menderes Massif, Turkey. I. The peristerite gap with coexisting kyanite. *Journal of Metamorphic Geology* **3**, 207–218.

Ashworth, J. R. & Evirgen, M. M. (1985b). Plagioclase relations in pelites, central Menderes Massif, Turkey. II. Perturbation of garnet–plagioclase barometers. *Journal of Metamorphic Geology* **3**, 219–229.

Coggon, R. & Holland, T. J. B. (2002). Mixing properties of phengitic micas and revised garnet–phengite thermobarometers. *Journal of Metamorphic Geology* **20**, 683–696.

Delor, C. P., Burg, J. P. & Leyreloup, A. F. (1984). Staurolite producing reactions and geothermobarometry of a high pressure thermal aureole in the French Massif Central. *Journal of Metamorphic Geology* **2**, 55–72.

Engi, M., Todd, C. S. & Schmatz, D. R. (1995). Tertiary metamorphic conditions in the eastern Lepontine Alps. *Schweizerische Mineralogische und Petrographische Mitteilungen* **75**, 347–369.

Fuhrman, M. L. & Lindsley, D. H. (1988). Ternary-feldspar modeling and thermometry. *American Mineralogist* **73**, 201–215.

Ghent, E. D. & Stout, M. Z. (1981). Geobarometry and geothermometry of plagioclase–biotite–garnet–muscovite assemblages. *Contributions to Mineralogy and Petrology* **76**, 92–97.

Gordon, T. M., Ghent, E. D. & Stout, M. Z. (1991). Algebraic analysis of the biotite–sillimanite isograd in the File Lake area, Manitoba. *Canadian Mineralogist* **29**, 673–686.

Green, T. H. & Hellman, P. L. (1982). Fe–Mg partitioning between coexisting garnet and phengite at high pressure, and comments on a garnet–phengite geothermometer. *Lithos* **15**, 253–266.

Himmelberg, G. R., Brew, D. A. & Ford, A. B. (1991). Development of inverted metamorphic isograds in the western metamorphic belt, Juneau, Alaska. *Journal of Metamorphic Geology* **9**, 165–180.

Hodges, K. V. & Crowley, P. D. (1985). Error estimation in empirical geothermometry and geobarometry for pelitic systems. *American Mineralogist* **70**, 702–709.

Hoisch, T. D. (1990). Empirical calibration of six geobarometers for the mineral assemblage quartz + muscovite + biotite + plagioclase + garnet. *Contributions to Mineralogy and Petrology* **104**, 225–234.

Hoisch, T. D. (1991). Equilibria within the mineral assemblage quartz + muscovite + biotite + garnet + plagioclase, and implications for the mixing properties of octahedrally-coordinated cations in muscovite and biotite. *Contributions to Mineralogy and Petrology* **108**, 43–54.

Holdaway, M. J. (2000). Application of new experimental and garnet Margules data to the garnet–biotite geothermometer. *American Mineralogist* **85**, 881–892.

Holdaway, M. J. (2001). Recalibration of the GASP geobarometer in light of recent garnet and plagioclase activity models and versions of the garnet–biotite geothermometer. *American Mineralogist* **86**, 1117–1129.

Holdaway, M. J. & Mukhopadhyay, B. (1993). A re-evaluation of the stability relations of andalusite: thermochemical data and phase diagram for the alumino silicates. *American Mineralogist* **78**, 298–315.

Holdaway, M. J., Dutrow, B. L. & Hinton, R. W. (1988). Devonian and carboniferous metamorphism in west–central Maine: the muscovite–almandine geobarometer and the staurolite problem revised. *American Mineralogist* **73**, 20–47.

Hynes, A. & Forest, R. C. (1988). Empirical garnet–muscovite geothermometry in low-grade metapelites, Selwyn Range (Canadian Rockies). *Journal of Metamorphic Geology* **6**, 297–309.

Keller, L. M., De Capitani, C. & Abart, R. (2005). A quaternary solution model for white micas based on natural coexisting phengite–paragonite pairs. *Journal of Petrology* **46**, 2129–2144.

Kleemann, U. & Reinhardt, J. (1994). Garnet–biotite thermometry revised: the effect of Al^{VI} and Ti in biotite. *European Journal of Mineralogy* **6**, 925–941.

Krogh, J. E. & Råheim, A. (1978). Temperature and pressure dependence of Fe–Mg partitioning between garnet and phengite, with particular reference to eclogites. *Contributions to Mineralogy and Petrology* **66**, 75–80.

Lang, H. M. & Rice, J. M. (1985). Regression modelling of metamorphic reactions in metapelites, Snow Peak, Northern Idaho. *Journal of Petrology* **26**, 857–887.

McMullin, D. W. A., Berman, R. G. & Greenwood, H. J. (1991). Calibration of the SGAM thermobarometer for pelitic rocks using data from phase-equilibrium experiments and natural assemblages. *Canadian Mineralogist* **29**, 889–908.

Newton, R. C. & Haselton, H. T. (1981). Thermodynamics of the garnet–plagioclase–Al_2SiO_5–quartz geobarometer. In: Newton, R. C., Navrotsky, A. & Wood, B. J. (eds) *Thermodynamics of Minerals and Melts*. New York: Springer, pp. 131–147.

Pattison, D. R. M. (1992). Stability of andalusite and sillimanite and the Al_2SiO_5 triple point: constraints from the Ballachulish aureole, Scotland. *Journal of Geology* **100**, 423–446.

Rothstein, D. A. & Hoisch, T. D. (1994). Multiple intrusions and low-pressure metamorphism in the central Old Woman Mountains, south-eastern California: constraints from thermal modelling. *Journal of Metamorphic Geology* **12**, 723–734.

Spear, F. S. (1995). *Metamorphic Phase Equilibria and Pressure–Temperature–Time Paths. Mineralogical Society of America Monograph*, 2nd edn, pp. 799.

Todd, C. S. (1998). Limits on the precision of geobarometry at low grossular and anorthite content. *American Mineralogist* **83**, 1161–1167.

Wu, C. M. & Cheng, B. H. (2006). Valid garnet–biotite (GB) geothermometry and garnet–aluminum silicate–plagioclase–quartz (GASP) geobarometry in metapelitic rocks. *Lithos* **89**, 1–23.

Wu, C. M., Wang, X. S., Yang, C. H., Geng, Y. S. & Liu, F. L. (2002). Empirical garnet–muscovite geothermometry in metapelites. *Lithos* **62**, 1–13.

Wu, C. M., Zhang, J. & Ren, L. D. (2004a). Empirical garnet–muscovite–plagioclase–quartz geobarometry in medium- to high-grade metapelites. *Lithos* **78**, 319–332.

Wu, C. M., Zhang, J. & Ren, L.D. (2004b). Empirical garnet–biotite–plagioclase–quartz (GBPQ) geobarometry in medium- to high-grade metapelites. *Journal of Petrology* **45**, 1907–1921.